Wavelets on graphs with application to transportation networks

Dhanya Menoth Mohan[1], Muhammad Tayyab Asif[2], Nikola Mitrovic[3], Justin Dauwels[4] and Patrick Jaillet[5,6]

Abstract— The technological advancements in Intelligent Transport Systems have made it possible to acquire large amounts of traffic data in real-time. As a result, various data-mining techniques are being used to extract useful traffic patterns. The research presented in this article focuses on the detection of disruptive traffic events such as congestion. In most transportation studies, traffic parameters are typically modeled as time series. However, these techniques fail to incorporate the spatial dependencies between different traffic variables. In this work, the traffic quantities such as speeds are considered as the signals defined at the vertices of a network line graph. Furthermore, the graph wavelet operators are applied to the spatial signals to generate the wavelet coefficients at different wavelet scales. By analyzing these wavelet coefficients, useful information such as origin, propagation, and the span of traffic congestion are inferred.

For analysis, we consider two major expressways in Singapore. The analysis shows that the abrupt changes in the speed can be captured by using the wavelet coefficients at the higher scales. On the other hand, the high magnitude coefficients at the lower wavelet scales reflect the smooth flow of the traffic across the network.

I. INTRODUCTION

Intelligent Transport Systems (ITS) can play a vital role in developing sophisticated control strategies for optimal usage of the road infrastructure of a land-scarce city like Singapore. The technological advancements in ITS and sensor developments enabled the availability of extensive data related to the on ground traffic conditions. Consequently, data driven approaches are being widely used for applications such as traffic sensing, congestion control, traffic forecasting, and route guidance [1]–[5].

In this work, we focus on detecting disruptive traffic events such as unexpected traffic speed fluctuations, traffic slowdown, and congestion that hinder normal traffic flow. The early detection of such traffic events can be useful in issuing early warnings that will eventually help the drivers to plan alternate routes.

Previous studies have proposed various methods to detect congestion and other disruptive events. These methods include Principal Component Analysis (PCA), Robust Principal Component Analysis (RPCA), Fourier transform, and wavelets. However, such approaches typically model

[1]Dhanya Menoth Mohan, [2]Muhammad Tayyab Asif, [3]Nikola Mitrovic , and [4]Justin Dauwels are with the School of Electrical and Electronic Engineering, Nanyang Technological University, 50 Nanyang Avenue, Singapore 639798 (dhanya001@e.ntu.edu.sg, muhammad89@e.ntu.edu.sg, nikolamitrovic84@gmail.com, and jdauwels@ntu.edu.sg).

[5]Patrick Jaillet is with the Laboratory for Information and Decision Systems, MIT, Cambridge, MA, 02139 (jaillet@mit.edu).

[6]Patrick Jaillet is also with the Center for Future Urban Mobility, Singapore-MIT Alliance for Research and Technology, Singapore.
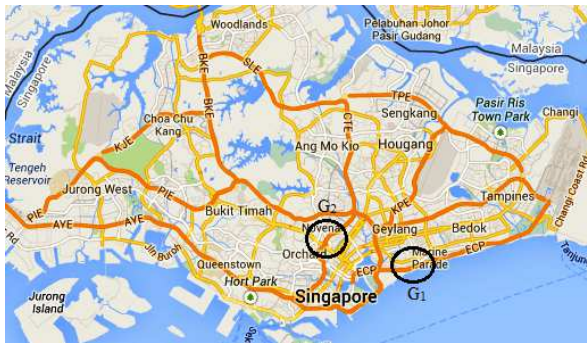
traffic parameters such as speed and flow as time series variables [6]–[12], [12]–[20]. In [6], Lakhina et al. applied PCA to generate subspaces of normal and abnormal traffic conditions in the communication network. Further, they used Fourier and exponential weighted moving average schemes to detect anomalies. The major drawback of the conventional PCA based detection systems is that it is not robust to the outliers. Moreover, tuning the parameters such as dimensionality of the normal subspaces and the detection threshold is challenging as it leads to high false-positive alarms [21].

Yang et al. proposed Coupled Bayesian Robust Principal Component Analysis for road traffic event detection which is an extension to Bayesian RPCA [7]. This method couples multiple data streams of nearby sensors so that they share a sparse structure. Furthermore, they used sparsity sharing to detect events in space and time. However, the data from different sensors were modeled as time series. Kerner et al. used Floating Car Data (FCD) to detect congestion in a traffic network [22]. This method relies on the collection and processing of travel time data sent by the FCD vehicles. The emergence and dissolution of congestion is detected by assessing the increase and decrease in the travel time on different road segments respectively. Thajchayapong et al. proposed a traffic anomaly detection and classification algorithm that utilizes the temporal changes in variance and the changes in spatial covariances of microscopic traffic variables [23].

Wavelet transforms have also been used for anomaly detection with applications to the communication networks. However, the variables are modeled as time series. We would refer to these techniques as classical wavelet transforms. For instance, Huang et al. had studied the network traffic anomaly detection problem in the temporal domain with the aid of classical wavelet transforms [8]. Barford et al. used similar techniques for Internet Protocol (IP) flow and Simple Network Management Protocol (SNMP) measurements to evaluate denial-of-service (DoS) attack and other abnormal events [9]. The authors in [24] proposed undecimated discrete wavelet transform and Bayesian analysis to detect network anomalies by considering the time-varying nature of the data. In addition, Xunyi et al. in [10], and Handi and Boudriga in [11] used classical wavelets to detect DoS attacks.

Other time series based detection systems are based on supervised learning [12]–[14], unsupervised learning [15]–[19], and Time-based Inductive learning Machine (TIM) [20]. Heller et al. in [12] proposed One Class Support Vector Machine (OCSVM) to identify anomalous windows

Fig. 1: The map G for wavelet analysis displaying the subnetworks G_1 and G_2.

Fig. 2: The subnetwork G_1 showing road segments from East Coast Parkway.

Fig. 3: The subnetwork G_2 showing road segments from Central Expressway.

registry access. This method constructs a model from the training data consisting of normal events and then classifies the test data as normal or anomalous. Lakhina et al. employed unsupervised learning techniques, i.e., clustering to classify the normal and disruptive events [15].

This paper proposes spectral graph wavelet transforms [25] for the detection of disruptive events such as traffic congestion. In contrast to the above mentioned time-series based approaches, the graph wavelet based method considers traffic parameters such as speed as the signal lying on the graph. It incorporates the relationship between the data defined over the network and the underlying topology; where the data is expected to be influenced by the network topology. Spectral graph wavelet transforms have been found application in areas such as transportation network, and neuronal network where network topology plays an important role [25], [26]. In this study, we apply this technique to road network.

In this method, we obtain scaling functions using the spectral decomposition of the discrete graph Laplacian ($\mathscr{L}$). This is done by calculating the eigenvalues and eigenvectors of $\mathscr{L}$. The graph Laplacian is the graph analogue to the Fourier transform. The wavelet operator T_g^s is then defined as $T_g^s = g(s\mathscr{L})$ for a given wavelet generating kernel g and scale parameter s. Furthermore, the wavelet coefficients are computed by applying this operator to the input graph signal defined at the vertices of the graph. These wavelet coefficients are then used to analyze the disruptive traffic events such as congestion.

Land Transport Authority (LTA) of Singapore provided the data for experimental purpose. The test network consists of expressway sections around the downtown area. With the help of spectral graph wavelet transforms, we would be able to detect the occurrence, spread, propagation, and the span of disruptive events.

The remainder of this paper is structured as follows. In Section II, we briefly describe spectral graph wavelet transforms. In Section III, we explain the data set. In Section IV, we describe and discuss how graph wavelets can be used to model events in the transportation network. In Section V, we provide concluding remarks.

II. SPECTRAL GRAPH WAVELET TRANSFORM - THEORETICAL OVERVIEW

In this section, we first review the theoretical aspects of classical wavelet transform, particularly, the Continuous Wavelet Transform (CWT). We then describe the forward transform, its inversion, and define scaling in Fourier domain. Finally, we discuss how these mathematical concepts and intuitions can be extended to signals defined on graphs. A more rigorous treatment on spectral graph wavelet transforms can be found in [25] and [26]. We will use the same notations as introduced in [25].

A. Classical Wavelet Transform

Classical wavelets $\psi_{s,a}$ of a function $f(x)$ at scale s and location a are constructed from the translated and scaled versions of the mother wavelet ψ:

$$\psi_{s,a}(x) = \frac{1}{s}\psi\left(\frac{x-a}{s}\right).$$

(1)

For a given function f, the wavelet coefficients $W_f(s,a)$ are calculated by convolving the input functions with the functions generated by the mother wavelet:

$$W_f(s,a) = \int_{-\infty}^{\infty} \frac{1}{s}\psi^*\left(\frac{x-a}{s}\right)f(x)dx.$$

(2)

The inverse CWT can be written as [27]:

$$f(x) = \frac{1}{\mathbf{C}_\psi}\int_0^\infty\int_{-\infty}^\infty W_f(s,a)\psi_{s,a}(x)\frac{dads}{s},$$

(3)

where $\mathbf{C}_\psi$ is defined as:

$$\mathbf{C}_\psi = \int_0^\infty \frac{|\psi(\omega)|^2}{\omega} d\omega < \infty, \tag{4}$$

where $\psi(\omega)$ is the Fourier transform of the mother wavelet $\psi(x)$. This equation is also called the admissibility condition.

It is challenging to directly apply the fundamental aspects of defining wavelets to the data defined over irregular, non-Euclidean spaces such as graph settings. In such settings, translation and contraction carry no meaning. An alternate way to perform Fourier transform on graphs is to use the so called Laplacian operators ($\mathscr{L}$) [25].

Before explaining the notion of the Laplacian operator, we will briefly discuss how scaling functions are defined in Fourier domain for the classical wavelet transform. We will also see how the resulting expression will help us to formulate an analogous transform on graphs. The wavelet transform for a fixed scale s may be considered as an operator T^s which takes the function f and returns the function $T^s f(a) = W_f(s,a)$. Here, the translation parameter is considered as the independent variable of the function returned by the operator [25]. Therefore,

$$\bar{\psi}_s(x) = \frac{1}{s} \psi^* \left(\frac{-x}{s} \right). \tag{5}$$

The operator T^s can be expressed as:

$$(T^s f)(a) = \int_{-\infty}^{\infty} \frac{1}{s} \psi^* \left(\frac{x-a}{s} \right) f(x) dx \tag{6}$$

$$= \int_{-\infty}^{\infty} \bar{\psi}_s(a-x) f(x) dx$$
$$= (\bar{\psi}_s \star f)(a).$$

By taking the Fourier Transform and applying the convolution theorem, we get:

$$\widehat{T^s f}(\omega) = \hat{\bar{\psi}}_s(\omega) \hat{f}(\omega). \tag{7}$$

Taking into account the scaling properties of the Fourier Transform and (5), we arrive at the following expression:

$$\hat{\bar{\psi}}_s = \hat{\psi}^*(s\omega). \tag{8}$$

Combining (5), (6), and (7), and inverting the transform yields:

$$(T^s f)(x) = \frac{1}{2\pi} \int_{-\infty}^{\infty} e^{i\omega x} \hat{\psi}^*(s\omega) \hat{f}(\omega) d\omega. \tag{9}$$

The scaling s appears only in the argument of $\hat{\psi}^*(s\omega)$, implying that the scaling can be defined in Fourier domain. The expression is used to derive spectral graph wavelet transforms discussed later in this section.

B. Weighted Graph and Graph Signal

1) Weighted Graph: Consider a connected, weighted graph $G = \{V, E, w\}$ with a set of vertices V, $|V| = N < \infty$, a set of edges E, and weight function $w : E \to \mathbb{R}^+$. The adjacency matrix A for the weighted graph G is the $N \times N$ matrix with entries $a_{m,n}$ where

$$a_{m,n} = \begin{cases} w(e) & \text{if } e \in E \text{ connects the vertices m and n} \\ 0 & \text{otherwise.} \end{cases} \tag{10}$$

The edge weights are defined by using a thresholded Gaussian kernel weighting function. Moreover, it reflects similarity or strength of correlation between the signals defined on vertex m and n.

2) Graph Signal: A graph signal is defined as a collection of a finite number of samples, each defined at the vertices of the graph and is represented as $f : V \to \mathbb{R}^N$, where the mth component of the signal f represents the traffic speed value at the mth vertex in V. For a road network, the signal on each vertex is the average speed on a particular road during a certain time interval. For our data set, the interval is 5 minutes.

C. Graph Laplacian

The non-normalized graph Laplacian is defined as $\mathscr{L} = D - A$, where the diagonal matrix D denotes the degree matrix. The mth diagonal element d_m of D is equal to the sum of the weights of all edges incident to the vertex m. For any signal $f \in \mathbb{R}^N$, $\mathscr{L}$ satisfies:

$$(\mathscr{L}f)(m) = \sum_{m \sim n} w_{m,n} \cdot [f(m) - f(n)], \tag{11}$$

where $m \sim n$ represents all vertices n that are connected to the vertex m. The eigenvectors χ_l satisfying:

$$\mathscr{L}\chi_l = \lambda_l \chi_l, \tag{12}$$

for $l = 0, 1, \ldots, N-1$ are associated with real, non-negative eigenvalues, $\{\lambda_l\}_{l=0,1,\ldots,N-1}$.

The entire spectrum is thus denoted by $\sigma(\mathscr{L}) = \{\lambda_0, \lambda_1, \ldots, \lambda_{N-1}\}$. In any graph, the Laplacian eigenvectors are analogous to the Fourier vectors and its eigenvalues, the frequencies [25].

D. Graph Fourier Transform

The classical Fourier Transform:

$$\hat{f}(\xi) = \langle f, e^{2\pi i \xi x} \rangle = \int_{\mathbb{R}} f(x) e^{-2\pi i x \xi} dx, \tag{13}$$

is the expansion of a function f in terms of complex exponentials. These exponentials are the eigenfunctions of the one-dimensional Laplacian operator $\frac{d^2}{dx^2}$. The graph Fourier transform can be defined in a similar manner using the graph Laplacian eigenvectors. Hence, the graph Fourier transform $\hat{f}$ of any function $f \in \mathbb{R}^N$ on the vertices of G:

$$\hat{f}(l) = \langle \chi_l, f \rangle = \sum_{n=1}^{N} \chi_l^*(n) f(n), \tag{14}$$

is an expansion of f in terms of the graph eigenvectors of the graph Laplacian. The inverse graph Fourier transform is thus determined as:

$$f(n) = \sum_{l=0}^{N-1} \hat{f}(l)\chi_l(n). \quad (15)$$

E. Spectral Graph Wavelet Transform

The spectral graph wavelet transform is generated by operator-valued functions of the Laplacian, called wavelet operators. The wavelet operator at scale s, for a wavelet generating kernel g, is defined as $T_g^s = g(s\mathscr{L})$. The wavelet operator $T_g = g(\mathscr{L})$ at scale $s = 1$ acts on a given function f by modulating each Fourier mode as:

$$\widehat{T_g f}(l) = g(\lambda_l)\hat{f}(l). \quad (16)$$

On applying inverse Fourier transform, we get

$$(T_g f)(m) = \sum_{l=0}^{N-1} g(\lambda_l)\hat{f}(l)\chi_l(m). \quad (17)$$

The kernel g is analogous to wavelet function $\hat{\psi}^*$ in (7). It should be noted that the kernel g is defined in the continuous domain even though the spatial domain for the graph is discrete. Thus, the scaling can assign any positive real number s.

The spectral graph wavelets are calculated by applying the wavelet operator to a delta impulse δ_n at a single vertex n as given below:

$$\psi_{s,n} = T_g^s \delta_n, \quad (18)$$

which yields:

$$\psi_{s,n}(m) = \sum_{l=0}^{N-1} g(s\lambda_l)\chi_l^*(n)\chi_l(m). \quad (19)$$

Finally the wavelet coefficients of the function f is calculated by performing the inner product with the individual graph wavelets as:

$$W_f(s,n) = \langle \psi_{s,n}, f \rangle. \quad (20)$$

On the other hand, the wavelet coefficients can directly be generated from wavelet operators (see (17)) by making use of the orthonormality of the eigenvectors χ_l. It is given as:

$$W_f(s,n) = (T_g^s f)(n) = \sum_{l=0}^{N-1} g(s\lambda_l)\hat{f}(l)\chi_l(n). \quad (21)$$

III. EXPERIMENTAL DATA

The road network G considered in this study comprises of several expressways and downtown roads in Singapore (Fig. 1). We use the data provided by LTA for the month of August 2011. The data set contains average speed values for individual links (road segments) sampled at 5 min intervals. These speed values represent the average speed of all the vehicles traversing the road segment during the given sampling interval.

The graph G is the network line graph where the variables are defined on the vertices or nodes. In the line graph, each

(a) wavelet traces: ECP-1. (b) wavelet traces: ECP-2.

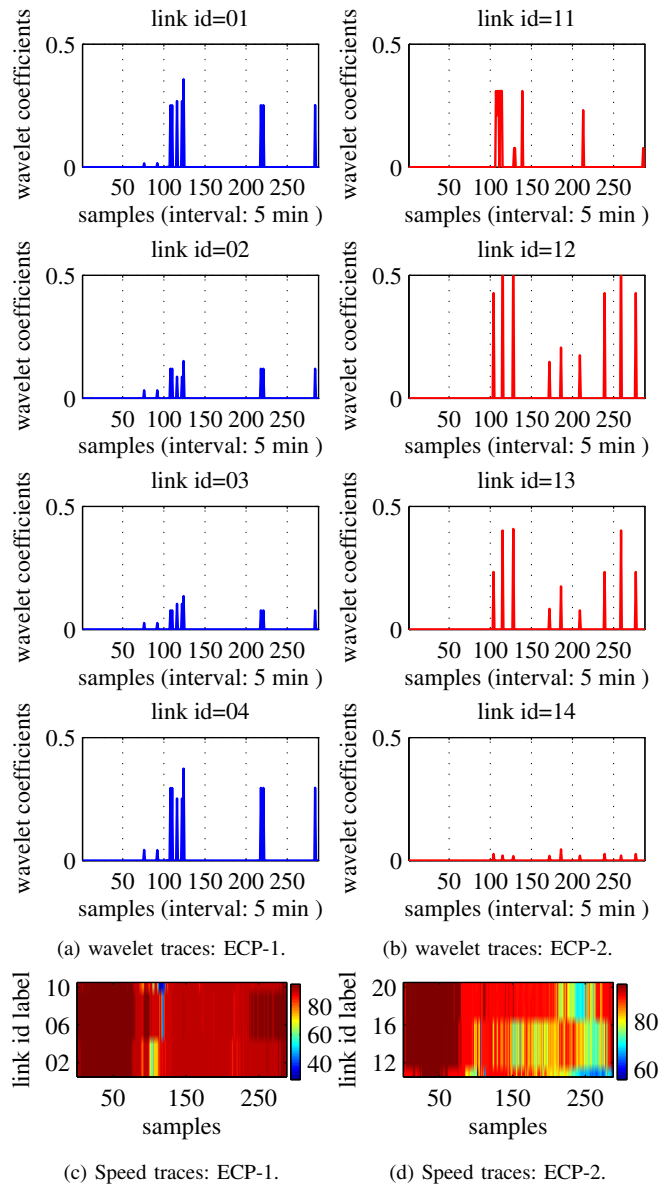(c) Speed traces: ECP-1. (d) Speed traces: ECP-2.

Fig. 4: One-day traffic wavelet traces ($s = 5$) for ECP in either direction ((a) and (b)). The average spatial traffic speed profiles (km/h) for each road (vertex) are given in (4c) and (4d) respectively.

road segment is represented by a vertex. If the two road segments m and n are connected with each other such that a vehicle can go from m to n, then an edge will exist between the nodes m and n in the line graph G. For convenience, we will refer a road segment as link.

For demonstration purposes, we consider the road segments from East Coast Parkway (ECP) and Central Expressway (CTE) (see Fig. 2 and Fig. 3). These two expressways are among the busiest roads of Singapore.

We apply graph wavelets to illustrate the variations in the traffic conditions during the whole day (speed values sampled at 5 min intervals from 12:00 a.m. to 11:55 p.m.).
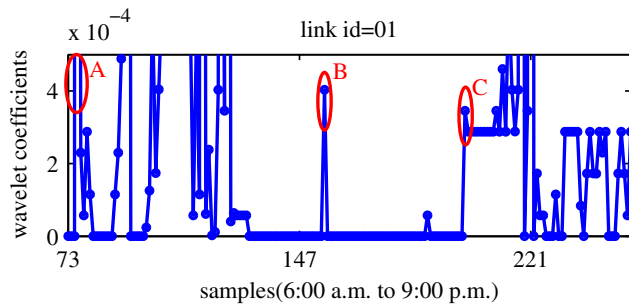
Fig. 5: The graph wavelet decomposition for an example link 01 from subnetwork G_1. The high magnitude variation corresponds to speed fluctuations. The anomaly is indicated in Red. A and C indicate the start of the morning and evening congestions respectively. B is another anomaly that occurred at sample 154 (Time: $12 : 45$ p.m.).

(a) wavelet traces: CTE link-24.

(b) wavelet traces: ECP link-01.

(c) Speed traces: CTE subnetwork consisting of link ids 20,21,...,28.

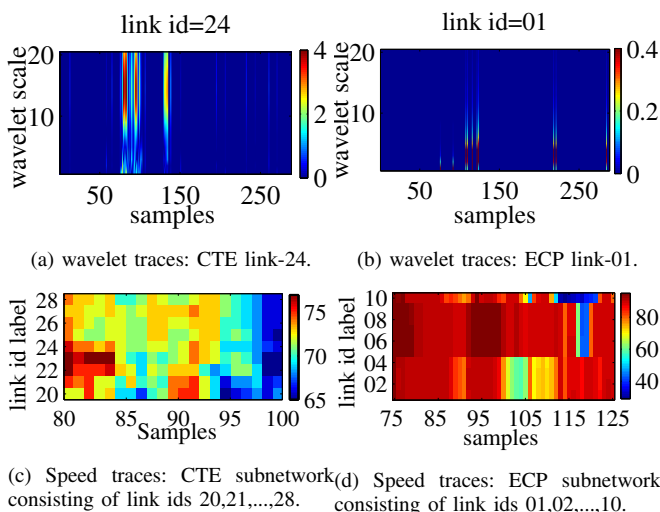(d) Speed traces: ECP subnetwork consisting of link ids 01,02,...,10.

Fig. 6: Wavelet coefficients during traffic congestion and normal flow. The wavelet decomposition for a sample traffic link affected by congestion in CTE and the corresponding speed traces of the subnetwork during the affected time (from 06:35 a.m. (sample=80) to 08:15 a.m. (sample=100)) are given in (6a) and (6c) respectively. The wavelet traces for ECP link during normal traffic and the corresponding speed traces (from 06:10 a.m. (sample=75) to 10:20 a.m. (sample=125)) of the subnetwork are given in (6b) and (6d).

IV. RESULTS AND DISCUSSIONS

In this section, we demonstrate how graph wavelets can be applied to detect disruptive traffic events in the network. For the sake of simplicity in visualization and interpretation, we restrict ourselves to two small subnetworks G_1 and G_2 (see Fig. 2 and Fig. 3). We employ the Spectral Graph Wavelets Toolbox (SGWT) [28] to implement the method outlined in Section II.

The traffic speed reported during the measurement period (12:00 a.m. to 11:55 p.m. with 5 min interval) is analyzed using graph wavelets at different scales $s = 1,2,..,20$.

Fig. 4a and Fig. 4b depict link level wavelet traces

of the ECP subnetwork in either direction. The wavelet decomposition at scale $s = 5$ of the graph signals (average speed) collected from individual links during the measurement period is also shown. The x-axis represents time instances of the day in terms of samples, i.e., 1 to 288 (here, the samples 1 and 288 correspond to 12:00 a.m. and 11:55 p.m. respectively). The magnitudes of the wavelet coefficients are plotted along the y-axis.

The high magnitude coefficients are observed to be concentrated in the vicinity of 08:15 a.m. (sample 100) and 06:40 p.m. (sample 225). These include the morning peak hours (7:00 a.m. to 9:00 a.m.) and the evening peak hours (5:00 p.m. to 7:00 p.m.). It can be seen from the Fig. 4c that the traffic speed across the links (link id 01, 02,...,10) drops to 40 km/h from a constant 80-85 km/h near the sample 125. Accordingly, the wavelet coefficients report high magnitude corresponding to this time instance, 10:20 a.m. (see Fig. 4a). The interesting point here is to note that the graph wavelets capture signal variation across the spatially related links rather than the variation at individual links (as in time-series based wavelet approach). In this way, it provides summarized information regarding the traffic condition in the network. Moreover, it avoids the necessity to analyze individual links in the network to infer and detect the event in the underlying network path. In addition, the graph wavelets report low magnitudes between sample 1 and 72 implying the absence of any unusual traffic speed variation during the time (12:00 a.m. to 05:55 a.m.). These findings further imply that the variations in the coefficient magnitude are the direct result of speed fluctuation across the network. Similar inferences can be made by analyzing the traffic flowing in the other direction (see Fig. 4b and Fig. 4d).

Once an unusual event (for example congestion) is detected in the network, it is possible to examine how it propagates through the neighboring links by analyzing that particular neighborhood. The wavelet decomposition for a set of topologically related links is displayed in Fig. 4a, and Fig. 4b. In Fig. 4a, the links 01, 02, and 03 show abnormal traffic between samples 100 and 125 (08:15 a.m. and 10:20 a.m.). It shows that the congestion originated in link 01 tends to propagate through link-02, link-03, and link-04. On the other hand, the congestion generated in link-11 vanishes from the neighborhood after traversing through link-12 and link-13. These results demonstrate how graph wavelets can be used to examine the propagation of the event detected (see Fig. 4a and Fig. 4b).

Next, to demonstrate the life span of an event, we perform link-level graph wavelet analysis. As shown in Fig. 5, the link exhibits anomaly traffic at 06:25 a.m. for a period of around 10 min (indicated as 'A'). Another abnormal event appeared at 12:45 p.m. spans for around 5 min ('B'). The tendency for the traffic to show significant variation becomes visible after 04:25 p.m. ('C').

Let us now discuss the significance of different wavelet scales in capturing the traffic trend of the network.

We further analyze the subnetworks in Fig. 2 and Fig. 3 at wavelet scales of $s =1$ to 20. The wavelet traces in Fig. 6a

are examined along with speed traces of the neighborhood (see Fig. 6c). The traffic speed variation across the links (link id=20, link id=22,..., link id=28) in the CTE subnetwork corresponding to the time from 06:35 a.m. to 08:15 a.m. (samples 80 to 100) during when the wavelet traces report unusual behavior is shown in Fig. 6c. It is to be noted that, from 06:35 a.m. to 08:15 a.m., the traffic speed across the links fluctuates between 65 km/hr and 75 km/hr. These fluctuations are picked up by the wavelets at higher scales. Thus, the higher scales capture the abrupt changes in the signal.

In contrast, the traffic speed varies smoothly across the links in the ECP subnetwork (see Fig. 6d) and therefore, the lower scale wavelet coefficients are large (see Fig. 6b). Thus, the lower scale wavelet coefficients capture the slow varying nature of the signal. These results demonstrate the significance of graph wavelet analysis with different scales to infer the nature of the disruptive event.

V. CONCLUSIONS AND FUTURE WORKS

In this work, we demonstrated the use of spectral graph wavelets to analyze unusual traffic conditions. To this end, we modeled traffic speed as a signal lying on a graph. The spectral graph wavelet transforms can be highly useful in understanding various characteristics of disruptive events such as traffic congestion. These characteristics include occurrence, spread, propagation, and span. In the future, the insights obtained from this study could be used for automatic event detection.

ACKNOWLEDGMENT

REFERENCES

[1] Z. Li, Y. Zhu, H. Zhu, and M. Li, "Compressive sensing approach to urban traffic sensing," in *Distributed Computing Systems (ICDCS), 2011 31st International Conference on*. IEEE, 2011, pp. 889–898.

[2] C. Y. Goh, J. Dauwels, N. Mitrovic, M. Asif, A. Oran, and P. Jaillet, "Online map-matching based on hidden markov model for real-time traffic sensing applications," in *Intelligent Transportation Systems (ITSC), 2012 15th International IEEE Conference on*. IEEE, 2012, pp. 776–781.

[3] Z. He, N. Jia, and W. Guan, "Route guidance strategies revisited: Comparison and evaluation in an asymmetric two-route traffic system," *arXiv preprint arXiv:1305.3009*, 2013.

[4] X. Fei, C.-C. Lu, and K. Liu, "A bayesian dynamic linear model approach for real-time short-term freeway travel time prediction," *Transportation Research Part C: Emerging Technologies*, vol. 19, no. 6, pp. 1306–1318, 2011.

[5] K. Chan, T. Dillon, J. Singh, and E. Chang, "Traffic flow forecasting neural networks based on exponential smoothing method," in *Industrial Electronics and Applications (ICIEA), 2011 6th IEEE Conference on*. IEEE, 2011, pp. 376–381.

[6] A. Lakhina, M. Crovella, and C. Diot, "Diagnosing network-wide traffic anomalies," in *ACM SIGCOMM Computer Communication Review*, vol. 34, no. 4. ACM, 2004, pp. 219–230.

[7] S. Yang, K. Kalpakis, and A. Biem, "Spatio-temporal coupled bayesian robust principal component analysis for road traffic event detection," 2013.

[8] P. Huang, A. Feldmann, and W. Willinger, "A non-instrusive, wavelet-based approach to detecting network performance problems," in *Proceedings of the 1st ACM SIGCOMM Workshop on Internet Measurement*. ACM, 2001, pp. 213–227.

[9] P. Barford, J. Kline, D. Plonka, and A. Ron, "A signal analysis of network traffic anomalies," in *Proceedings of the 2nd ACM SIGCOMM Workshop on Internet measurment*. ACM, 2002, pp. 71–82.

[10] X. Ren, R. Wang, and H. Wang, "Wavelet analysis method for detection of ddos attack on the basis of self-similarity," *Frontiers of Electrical and Electronic engineering in China*, vol. 2, no. 1, pp. 73–77, 2007.

[11] M. Hamdi and N. Boudriga, "Detecting denial-of-service attacks using the wavelet transform," *Computer Communications*, vol. 30, no. 16, pp. 3203–3213, 2007.

[12] K. Heller, K. Svore, A. D. Keromytis, and S. Stolfo, "One class support vector machines for detecting anomalous windows registry accesses," in *Workshop on Data Mining for Computer Security (DMSEC), Melbourne, FL, November 19, 2003*, 2003, pp. 2–9.

[13] T. Singliar and M. Hauskrecht, "Towards a learning traffic incident detection system," in *Proc. Workshop on Machine learning Algorithms for Surveillance and Event Detection*. Citeseer, 2006.

[14] A. B. Gardner, A. M. Krieger, G. Vachtsevanos, and B. Litt, "One-class novelty detection for seizure analysis from intracranial eeg," *The Journal of Machine Learning Research*, vol. 7, pp. 1025–1044, 2006.

[15] A. Lakhina, M. Crovella, and C. Diot, "Mining anomalies using traffic feature distributions," in *ACM SIGCOMM Computer Communication Review*, vol. 35, no. 4. ACM, 2005, pp. 217–228.

[16] G. Munz, S. Li, and G. Carle, "Traffic anomaly detection using k-means clustering," *Proc. of performance, reliable "a ssigkeits and Verl ä sslichkeitsbewertung of communication networks and distributed systems*, vol. 4, 2007.

[17] K. Leung and C. Leckie, "Unsupervised anomaly detection in network intrusion detection using clusters," in *Proceedings of the Twenty-eighth Australasian conference on Computer Science-Volume 38*. Australian Computer Society, Inc., 2005, pp. 333–342.

[18] M. F. Lima, B. B. Zarpelao, L. D. Sampaio, J. J. Rodrigues, T. Abrao, and M. Proenca, "Anomaly detection using baseline and k-means clustering," in *Software, Telecommunications and Computer Networks (SoftCOM), 2010 International Conference on*. IEEE, 2010, pp. 305–309.

[19] I. Syarif, A. Prugel-Bennett, and G. Wills, "Unsupervised clustering approach for network anomaly detection," in *Networked Digital Technologies*. Springer, 2012, pp. 135–145.

[20] H. S. Teng, K. Chen, and S. Lu, "Adaptive real-time anomaly detection using inductively generated sequential patterns," in *Research in Security and Privacy, 1990. Proceedings., 1990 IEEE Computer Society Symposium on*. IEEE, 1990, pp. 278–284.

[21] H. Ringberg, A. Soule, J. Rexford, and C. Diot, "Sensitivity of pca for traffic anomaly detection," in *ACM SIGMETRICS Performance Evaluation Review*, vol. 35, no. 1. ACM, 2007, pp. 109–120.

[22] B. Kerner, C. Demir, R. Herrtwich, S. Klenov, H. Rehborn, M. Aleksic, and A. Haug, "Traffic state detection with floating car data in road networks," in *Intelligent Transportation Systems, 2005. Proceedings. 2005 IEEE*. IEEE, 2005, pp. 44–49.

[23] S. Thajchayapong, E. S. Garcia-Treviño, and J. A. Barria, "Distributed classification of traffic anomalies using microscopic traffic variables," *Intelligent Transportation Systems, IEEE Transactions on*, vol. 14, no. 1, pp. 448–458, 2013.

[24] V. Alarcon-Aquino and J. A. Barria, "Anomaly detection in communication networks using wavelets," *IEE Proceedings-Communications*, vol. 148, no. 6, pp. 355–362, 2001.

[25] D. K. Hammond, P. Vandergheynst, and R. Gribonval, "Wavelets on graphs via spectral graph theory," *Applied and Computational Harmonic Analysis*, vol. 30, no. 2, pp. 129–150, 2011.

[26] D. I. Shuman, S. K. Narang, P. Frossard, A. Ortega, and P. Vandergheynst, "The emerging field of signal processing on graphs."

[27] A. Grossmann and J. Morlet, "Decomposition of hardy functions into square integrable wavelets of constant shape," *SIAM journal on mathematical analysis*, vol. 15, no. 4, pp. 723–736, 1984.

[28] D. K. Hammond. (2010) The spectral graph wavelets toolbox. [Online]. Available: http://wiki.epfl.ch/sgwt